

## POROUS PERMEABLE CERMET MATERIALS BASED ON IRON OXIDES WITH ADDITIONS OF GROUND POLYMETAL ORES

M. S. Kanapinov,<sup>1</sup> A. V. Maetskii,<sup>1,2</sup> A. A. Sitnikov,<sup>1</sup>  
N. P. Tubalov,<sup>1</sup> and V. V. Kovalev<sup>1</sup>

Translated from *Novye Ogneupory*, No. 7, pp. 58 – 65, July, 2018.

*Original article submitted December 7, 2017.*

Self-propagating high-temperature synthesis (SHS) is used to prepare heat-resistant porous permeable cermet material (PPCM) based on a mixture composed of alloy steel scale powder and oxides of metals and polymetal (monazite). The SHS-material obtained may be used as a catalytic agent for cleaning diesel exhaust gases. In this case instead of expensive rare-earth elements (REE) cerium and thorium ground complex ores containing these REE may be used. The effect of monazite content up to 18 wt.% in a charge on physicomaterial and service properties of the prepared materials is considered.

**Keywords:** porous permeable cermet material (PPCM), self-propagating high-temperature synthesis (SHS), SHS-material, monazite, SHS-filters, degree of exhausted gas cleaning.

### INTRODUCTION

The contemporary level of development of engineering with increased intensity of operating regimes for machines and equipment suggests expansion of refractory material and object production. These materials may be classified as porous permeable cermet materials (PPCM) that may be prepared using self-propagating high-temperature synthesis (SHS) [1 – 7]. Researchers of SHS [1 – 3] confirm the unique nature of conditions for the process and primarily high activity gradients in the combustion wave front ( $10^2 - 10^5 \text{ K}\cdot\text{sec}^{-1}$ ) and slow characteristic process times ( $10^{-2} - 10^{-1} \text{ sec}$ ). In this case alongside chemical kinetics component parts of the macrokinetics are processes of mass and heat transfer.

A typical powder SHS-system in the original condition is a porous heterogeneous material with a heterogeneity scale of 1 – 100  $\mu\text{m}$ . It follows from this that in describing for example processes of heat transfer in an SHS wave it is necessary to consider features of heat transfer in porous materials. Primarily these materials are distinguished by a variety of heat transfer mechanisms, including conduction (solid and

gas phase), convective, and radiant (radiation). It is well known that in powder materials with porosity of more than 30% (which is typical for the majority of original SHS-systems) mass transfer is accomplished (due to the high heat resistance of contacts between particles) not due to conduction through condensed phase, but through gas within pores (conduction of convection) and the role of the radiant component in overall heat transfer increases with an increase in pore size and amount.

Exhaust gases of internal combustion engines, used universally as energy installations of automobiles, tractors, river and marine transport vessels, and energy supply, contain up to 1200 different components, including toxic (carbon monoxide CO, nitrogen oxides  $\text{NO}_x$ , hydrocarbons  $\text{C}_x\text{H}_y$ , and solid particles SP). Currently for cleaning exhaust gases of heating units in objects (soot filters and catalytic neutralizers) four leading types of materials are used, prepared on the basis of metals, inorganic compounds, organic compounds, and composites. The material for gas cleaning exhibits of set of important physical physicomaterial, and functional properties [8 – 11].

The attraction of using SHS for preparing PPCM includes primarily the fact that instead preparing and cleaning rare-earth elements (REE), i.e., cerium, thorium, etc., by complex technology there is use of milling polymetal ore

<sup>1</sup> I. I. Polzunov Altai State Technical University, Barnaul, Russia.

<sup>2</sup> maetscky@yandex.ru

containing these REE. It is important for preparing high quality PPCM by the SHS method to select the original charge components. Currently the main charge for preparing porous materials is industrial waste of engineering enterprises, represented by oxides of metals (alloyed steel scale) metal powder, and polymetal ore, i.e., monazite, containing cerium and thorium [11].

The aim of the present work is development and preparation of PPCM by the SHS method with addition of monazite ore to a charge instead of expensive REE. This substitution will make it possible to provide the catalytic properties of PPCM as filters for fine cleaning of transport exhaust gases [11, 12].

## POWDER AND CHARGE PREPARATION

Preparation of the starting materials included crushing of alloy steel scale in a conical crusher and separation of fractions 50 – 125 μm on screens. Studies of the scale powder studied demonstrated that the predominant type of material breakdown is intercrystalline failure. In this case particles of the powder obtained of different fractions have similar morphology, repeating that of original material ferrite crystallites. There is typically sharp separation in powder product fraction composition corresponding to single crystallite and polycrystalline fragments of certain sizes. Before charge preparation for synthesis all powders of the starting components and alloyed steel scale were dried in a vacuum chamber at 345 – 355 K for 3 – 4 h. Powders were prepared from the selected fractions as a mixture of constant composition, from which subsequently PPCM specimens were prepared.

On the basis of experimental histograms for effective pore cross section distribution in specimens based on powder of each fraction [13], regression analysis methods were used to obtain the value of effective SHS material pore cross section:

$$D_{\text{ef}} = d(0.9 - 0.95), \quad (1)$$

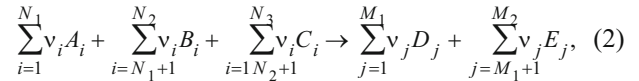
where  $D_{\text{ef}}$  is effective pore cross section, mm;  $d$  is particle cross section for fractions, mm.

Relationship (1) is fulfilled with a standard error of not more than 0.075 and correlation coefficient of 0.7.

## PPCM PREPARATION USING THE SHS PROCESS

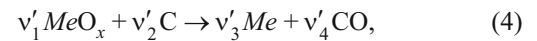
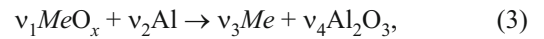
Charge material selection is of considerable importance for porous object preparation. A broad range of metal oxide mixtures is capable of burning with reducing agent and non-metal. Products of their combustion are carbides, borides, silicides, nitrides, porous and composite oxides, hard alloys, and cermets. For mixtures the thermal effect is more than 5 kJ/g, the combustion temperature exceeds the combustion product melting temperature, and therefore after crystallization they are obtained in cast form. The chemical scheme for

preparing porous refractory compounds and hard alloys may be presented in the form

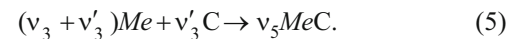


where  $A_i$  is original oxides ( $\text{Fe}_2\text{O}_3$ ,  $\text{Cr}_2\text{O}_3$ ,  $\text{CrO}_2$ ,  $\text{NiO}$ ,  $\text{Fe}_3\text{O}_4$ ,  $\text{FeO}$ , etc.);  $B_i$  are metal-reducers (Al, Ni, Cr, etc.);  $C_i$  are non-metals (C, Si,  $\text{SiO}_2$ , etc.);  $D_i$  are final combustion products ( $\text{Cr}_3\text{C}_2$ ,  $\text{Cr}_5\text{Al}_8$ ,  $\text{NiAl}$ ,  $\text{ThO}_2$ , Ce, etc.);  $E_i$  are metal-reducer oxides ( $\text{Al}_2\text{O}_3$ ,  $\text{Cr}_2\text{O}_3$ , etc.);  $\nu_i$  and  $\nu_j$  are stoichiometric coefficients for the original components and final products respectively.

According to this scheme, apart from carbides and oxides of metal reducing agents hard alloys, cermets, composite oxides, etc., are obtained. Generally it is possible to separate four main stages: combustion, phase separation, cooling and crystallization of molten products, and phase transitions. In the first stage two competing reactions proceed



and in the second there is carbidization of reduced metal



In the majority of cases reaction (3) is high-temperature ( $Q_2 \sim 4 \times 10^6$  J/kg), reaction (4) is endothermic ( $Q < 0$ ), i.e., only reaction (3) is the leading reaction at a combustion temperature of 1500 – 2200 K.

Having a number of common features with production processes of traditional powder metallurgy, SHS is characterized by such a unique feature as a marked high-temperature solid-liquid medium during occurrence of synthesis and permits different types of external action, by means of which it is possible to control the structure and properties of finished products. In our case at the basis of SHS is the reaction of exothermic interaction of two or several chemical elements, compounds, occurring within a directional combustion regime. The SHS process is accomplished within a thin layer of mixture of starting reagents after local initiation of a reaction and propagation throughout the whole system due to heat transfer from the burning products to “unheated” starting material. In this case cermet materials are obtained with a porous structure [14, 15] that from due to melt redistribution within a reaction zone and gas desorption [16, 17].

## BASIC MATERIAL

Proceeding from provision of physicomechanical and functional indices (elasticity modulus, mechanical stresses in bending and compression) a basic charge composition has

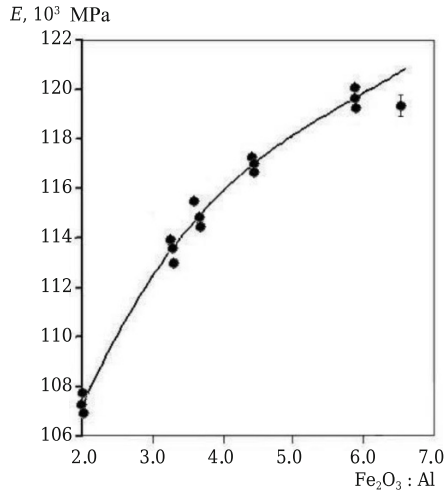


**Fig. 1.** Dependence of PPCM elasticity modulus  $E$  on  $\text{Fe}_2\text{O}_3:\text{Al}$  ratio in a charge.

been developed, wt.%: alloyed steel 18Kh2N4MA scale 30–60;  $\text{Al}_2\text{O}_3$  (corundum) 30–45; aluminum ASD-1 8–15. Scale in the form of powder fraction 60–125  $\mu\text{m}$ , and electrocorundum and aluminum as fractions 50–60  $\mu\text{m}$  were used. In this case grain shape was round (an angular shape of grains has insufficient reaction capacity that wors-

ens final product quality). The quantitative ratio of starting materials was taken from calculation of thermal synthesis at 950–1050°C without melting charge components.

Reaction of aluminum with scale proceeds by reaction (2). The scale phase composition, determined by x-ray phase quantitative analysis, includes 58–59% iron (II) oxide, 40–48% iron (ferrite), and 1.5–2.0% oxides of alloying elements. In original plates of scale the starting components melt at the surface and in a surface layer with depth up to 25  $\mu\text{m}$  (measured in a specially prepared transverse microsection of a scale plate, and a deeper layer formed by ferrite). The process of steel hot treatment, accompanied by scale formation, is quite short term, and ferrite does not experience internal oxidation. A typical feature of the SHS process with a basic charge composition  $\text{Fe}_2\text{O}_3 + \text{Al}_2\text{O}_3 + \text{Al}$  is formation of a ceramic framework of crystalline  $\text{Al}_2\text{O}_3$  [8–10]. Simultaneously there is reduction of iron followed by coalescence of iron liquid phase around a solid framework of  $\text{Fe}-\text{Fe}_3\text{O}_4-\text{Al}_2\text{O}_3$ . These macro-formations as a result of intense heat liberation and gas distribution change shape and increase pore size.

During SHS redistribution of crystal structure atoms proceeds on scales of the order of interatomic distances, i.e., so-called phase ordering transitions arise. The crystal lattice of a disordered phase breaks down into several sub-lattices, in each of which concentration differs from the average for

**TABLE 1.** Charge Composition with Addition of Monazite, Physicomechanical and Functional Properties of Porous Permeable SHS-Materials

Properties	SHS-material version			
	M-1	M-2	M-3	M-4
<i>Composition, wt.%:</i>				
alloy steel (18KhNVA, 18KhNMA, 40KhNMA, etc.)	49.5	49.5	49.5	49.5
scale and electrocorundum in equal amounts				
chromium oxide	12.0	11.5	11.0	10.5
chromium PKh-1 by TU 882–76	6.0	5.6	5.4	5.2
nickel PNK-OT-1 by GOST 9722–79	6.1	6.0	5.7	5.4
aluminum ASD-1 by TU 485-22–87	12.4	12.4	12.4	12.4
monazite	14	15	16	17
<i>Physicomechanical characteristics</i>				
Average derived pore diameter, $\mu\text{m}$	123	130	142	168
Pore sinuosity with $\delta_{st} = 10 \text{ mm}$	1.15	1.21	1.27	1.32
Specific surface, $\text{m}^2/\text{g}$	86	94	107	126
Porosity	0.45	0.50	0.54	0.55
Air permeability, $10^{-12} \text{ m}^2$	1.32	1.42	1.71	2.13
<i>Ultimate strength, MPa:</i>				
in compression	10.5	8.3	6.4	4.3
in bending	8.0	6.5	5.0	3.5
Impact strength, $\text{J}/\text{m}^2$	0,282	0,275	0,260	0,235
Corrosion resistance, %	13.5	14.8	15.2	16.4
<i>Functional properties</i>				
<i>Concentration reduction, %:</i>				
CO	62	68	64	80
$\text{NO}_x$	42	49	55	68
$\text{C}_x\text{H}_y$	62	68	73	84
TU	90	91.5	94.8	99

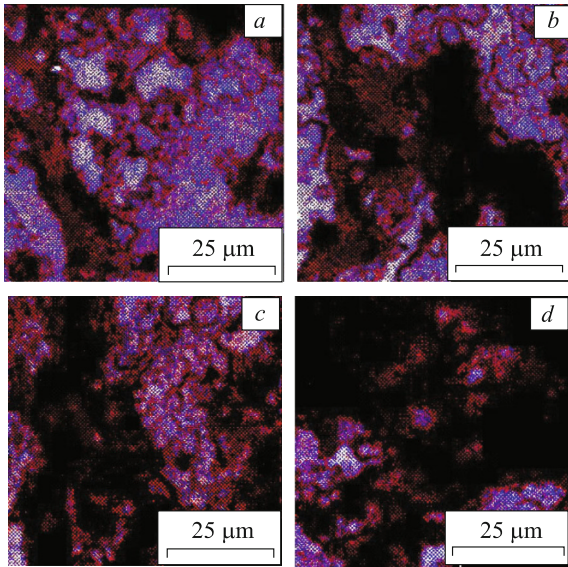


**Fig. 2.** SHS-material microstructure with addition of monazite: a) composition M-1; b) composition M-2; c) composition M-3; d) composition M-4 (see Table 1).

the alloy. In actual Fe–Al alloys transition into this phase with a reduction in temperature proceeds in two stages. At first at high temperature there is phase ordering transition (FeAl → Fe<sub>3</sub>Al). According to the composition diagram for the Fe–Al system aluminum forms solid solutions, intermetallic compounds, and eutectic with iron. In the system solid phases Fe<sub>3</sub>Al (β<sub>1</sub>), FeAl (β disordered, β<sub>2</sub> ordered) Fe<sub>2</sub>Al<sub>3</sub> (ε), FeAl<sub>2</sub> (ξ), FeAl<sub>3</sub> (θ), Fe<sub>3</sub>Al<sub>5</sub> (η) exist. An advantage of alloys based on Fe<sub>3</sub>Al is high resistance against oxidation and sulfide corrosion, and a deficiency gives low-temperature brittleness, caused by alloy saturation with hydrogen, formed during reaction of aluminum with water vapor from air moisture, present within the composition of corundum crystals. The porous material obtained intended as a filter element has an ultimate strength in compression of 2 – 7 MPa, overall porosity of about 50%, and communication between pores of round and longitudinal shape with a size of 20 – 200 μm, but could reach up to 400 μm.

It should be noted that PPCM charge compositions are basic, and they differ in the weight fractions of aluminum and iron oxides. A dependence has been obtained for elasticity modulus of PPCM on the ratio Fe<sub>2</sub>O<sub>3</sub>:Al in a charge (Fig. 1). Experimental data have made it possible to determine the physicomechanical properties and frequency of natural variations of PPCM specimens in relation to the Fe<sub>2</sub>O<sub>3</sub>:Al ratio in a charge.

**PPCM using polymetal ore milling**

The prerequisites for using monazite for preparing catalytic materials by the SHS method are:

- monazite is quite widespread and is an associated material in volcanic and metamorphic rocks, and gold-bearing

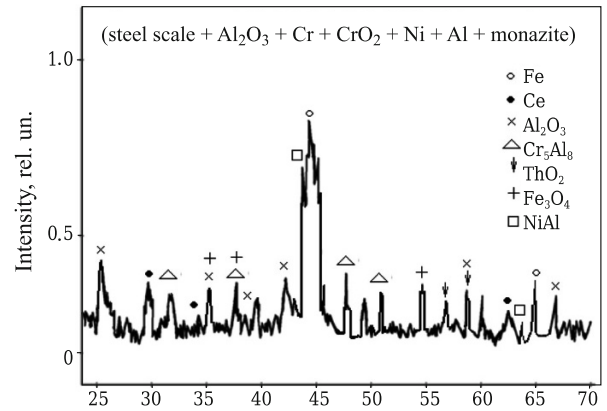


**Fig. 3.** SHS-material containing monazite (composition M-4, see Table 1) diffraction pattern.

veins. It is a phosphate of the cerium group of lanthanoids and normally contains small amounts of Ce, Th, etc.;

- use within a charge composition of Cr, Cr<sub>2</sub>O<sub>3</sub>, CrO<sub>2</sub>, Ni, Ce, and Th proposed for preparing SHS alloys are catalysts for oxidation of incomplete fuel combustion products.

In addition, during preparation of filters for cleaning engine exhaust gases it is necessary to consider both the composition of the gases being filtered and their temperature (120 – 750°C), presence of free oxygen, and corrosive components of the nitrogen and carbon, and sulfur oxide types. Since ThO<sub>2</sub> is within monazite, being a refractory material, then this additionally provides the required operating properties of a filter for diesel exhaust gases. Data about the composition of charges with addition of monazite, and also the physicomechanical and functional properties of SHS materials are provided in Table 1. The microstructure of materials with addition of monazite is shown in Fig. 2, and x-ray diffraction pattern of SHS material (M-4) containing 17% monazite in a charge is shown in Fig. 3. For comparison charge compositions are indicated below containing cerium and thorium, and also the properties of the materials obtained:

<i>Composition, wt. %:</i>	
alloy steel (18KhNVA, 18KhNMA, 40KhNMA, etc.)	
scale and electrocorundum in equal amounts	49.5
chromium oxide	18
chromium PKh-1	6.9
nickel PNK-OT-1	12.4
aluminum ASD-1	12.9
cerium	0.2
thorium	0.1
<i>Physical characteristics</i>	
Average derived pore diameter, μm	155
Pore sinuosity with δ <sub>st</sub> = 10 mm	1.18
Specific surface, m <sup>2</sup> /g	108
Porosity	0.42
Air permeability, 10 <sup>-12</sup> m <sup>2</sup>	2.31
<i>Physicomechanical characteristics</i>	
Ultimate strength, MPa:	
in compression	9.6
in bending	3.2



Impact strength, J/m <sup>2</sup> . . . . .	0.275
Corrosion resistance, % . . . . .	13
<i>Functional properties</i>	
Concentration reduction, %:	
CO . . . . .	84
NO <sub>x</sub> . . . . .	50
C <sub>x</sub> H <sub>y</sub> . . . . .	58
TU . . . . .	91

Values of the double diffraction angle 2θ and interplanar distances *d* (*d*<sub>st</sub> is standard value, *d*<sub>ex</sub> is experimental value) using a diffraction maximum for Fe as equal to 1, are given in Table 2.

The possibilities detected for controlling material porosity and pore diameter provide a precedence for regulating these parameters during creation of new materials by dispensing monazite into the charge composition in order to prepare materials using SHS. Complex actions due to changing both composition and production regimes are possible. With an increase in monazite content *C*<sub>mnz</sub> in a material charge there is an increase in pore sinuosity ξ<sub>s</sub>, which is important in controlling material properties in the early stages during determination of charge composition. From results of experimental studies a change in pore sinuosity has been obtained in relation to monazite content within a charge. This relationship has been described by us as a linear expression

$$\xi_s = 0.0529 \cdot C_{mnz} + 0.4159. \quad (6)$$

An increase in pore sinuosity with an increase in monazite addition to a charge is explained by an increase in the proportion of inert materials, both participating in high-temperature synthesis, and burning off during the process. In this case pore sinuosity starts to appear both due to formation of “cavernous” cavities, and due to an increase in pore internal roughness. However, in all cases a layered structure of the material framework remains almost un-

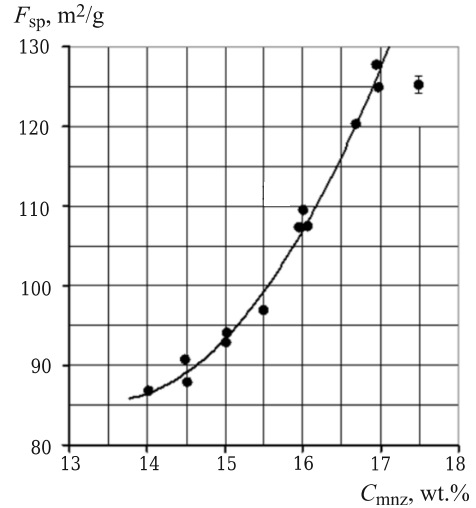


Fig. 4. Effect of *C*<sub>mnz</sub> in charge on *F*<sub>sp</sub> of SHS-material.

changed with the position of sinuous pores almost perpendicular to the SHS wave front advance. Development of pore diameter and their sinuosity with an increase in charge monazite content leads to an increase in material specific surface. It should be noted that in creating specific surface there also participation of micropores within material. Monazite participates in metal-reduction processes with steel scale. An experimental study has shown that the dependence of specific surface for porous permeable SHS catalytic materials on charge monazite content is not linear in nature (Fig. 4). Appearance of cracks and blowholes in porous material with a monazite concentration of more than 16.5% facilitates an increase in diffusion processes during gas cleaning.

TABLE 2. Values of 2θ and *d* for Different SHS-Product Phases

2θ, deg	<i>d</i> <sub>st</sub> , Å	<i>d</i> <sub>exp</sub> , Å	2θ, deg	<i>d</i> <sub>st</sub> , Å	<i>d</i> <sub>exp</sub> , Å
	Fe (6 – 696)*			ThO <sub>2</sub> (2 – 1278)	
44.673	2.0268	2.03	54.231	1.69	1.70
65.021	1.4332	1.43	57.231	1.61	1.60
	F <sub>3</sub> O <sub>4</sub> (1 – 111)			Cr <sub>5</sub> Al <sub>8</sub> (29 – 15)	
35.451	2.53	2.50	33.862	2.645	2.66
37.120	2.42	2.40	37.104	2.421	2.40
53.546	1.71	1.70	47.318	1.7654	1.7654
	Al <sub>2</sub> O <sub>3</sub> (5 – 712)			NiAl (44 – 1188)	
25.584	3.479	3.48	51.739	1.9195	1.92
35.136	3.552	2.56	44.377	2.0413	2.04
37.784	2.379	2.38	64.549	1.4437	1.44
43.361	2.085	2.08		Ce (1 – 887)	
57.518	1.601	1.60	30.088	2.97	2.95
66.546	1.404	1.40	34.911	2.57	2.60
			59.651	1.55	1.57

\* Figures in brackets here and subsequently signify temperature range, K, within which SHS-product retains a phase in question.

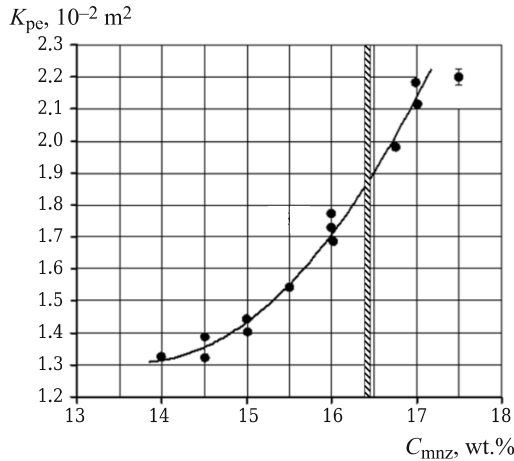


Fig. 5. Effect of  $C_{mnz}$  on  $K_{pe}$  of SHS-material.

As a result of mathematical treatment of experimental material and expression has been obtained describing the dependence of specific surface  $F_{sp}$  on  $C_{mnz}$  in a charge for preparing porous SHs catalytic material:

$$F_{sp} = 3.3759 \cdot C_{mnz}^2 - 91.018 \cdot C_{mnz} + 699.03. \quad (7)$$

A dependence is shown in Fig. 5 for permeability  $K_{pe}$  of porous material with respect to air on monazite content in an original charge composition. Treatment of research results has made it possible to obtain an expression describing this functional connection:

$$K_{pe} = 0.0775 \cdot C_{mnz}^2 - 2.1292 \cdot C_{mnz} + 15.928 \times 10^{-12}. \quad (8)$$

An increase in charge monazite content has a significant effect on mechanical strength of SHS material (Fig. 6). It has been established that an increase in  $\text{Cr}_2\text{O}_3$  content in charge from 14 to 17% leads to a reduction in ultimate strength in compression  $\sigma_{co}$  from 10.5 to 4.5 MPa, or by a factor of 2.33. In this case the ultimate strength in bending  $\sigma_{ben}$  decreases from 8.0 to 3.5 MPa, or by a factor of 2.28. This is explained by the fact that between refractory metal particles and dissolved melts of readily melting metals there is formation of a phase containing oxides. On the basis of results of treating experimental data expressions have been obtained describing the dependence of  $\sigma_{co}$  and  $\sigma_{ben}$  on monazite content in charge of an SHS system:

$$\sigma_{co} = -2.0238 \cdot C_{mnz} + 38.636, \quad (9)$$

$$\sigma_{ben} = -1.4708 \cdot C_{mnz} + 28.578. \quad (10)$$

The reduction observed in  $\sigma_{co}$  and  $\sigma_{ben}$  with an increase in  $C_{mnz}$  in a charge of an SHS system is reflected in the change in impact strength  $v_{im}$  for materials. With an increase

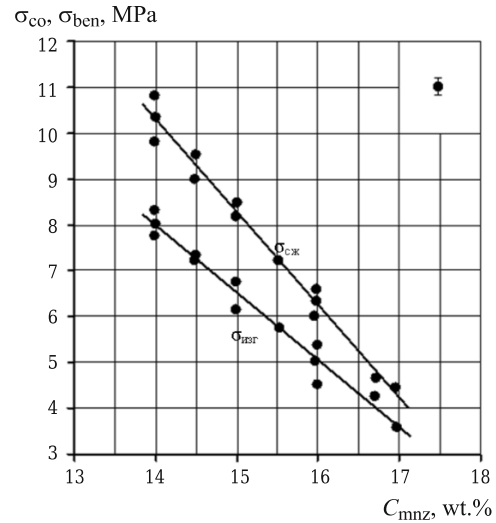


Fig. 6. Dependence of SHS-material mechanical strength on  $C_{mnz}$ .

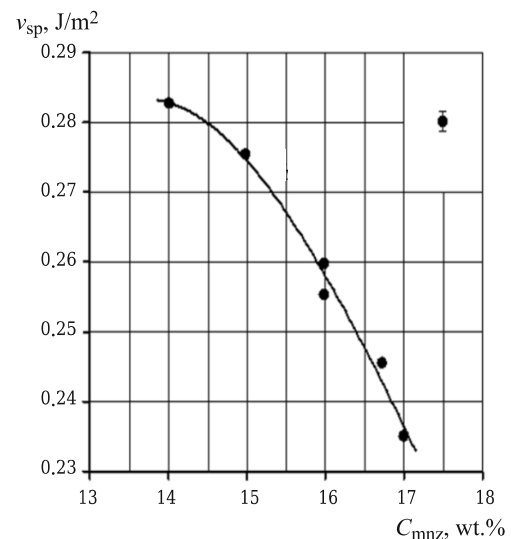


Fig. 7. Effect of monazite content in charge on SHS-material  $v_{sp}$ .

in  $C_{mnz}$  from 14–17%  $v_{sp}$  decreases from 0.282 to 0.235  $\text{kJ/m}^2$ , or by a factor of 1.2 (Fig. 7). An expression has been obtained connecting  $v_{sp}$  with  $C_{mnz}$ :

$$v_{sp} = -0.0033 \cdot C_{mnz}^2 + 0.085 \cdot C_{mnz} - 0.272. \quad (11)$$

Analysis of experimental data shows that with an increase in pore diameter, sinuosity, and development of specific material surface is mechanical strength decreases.

Dependences are shown in Fig. 8 for cleaning quality  $\delta$  for gases on monazite content in a charge, and also the boundary within whose limits porous SHS materials do not have cracks and blowholes. Gas cleaning quality from TP with a change in monazite content from 14 to 17% increases

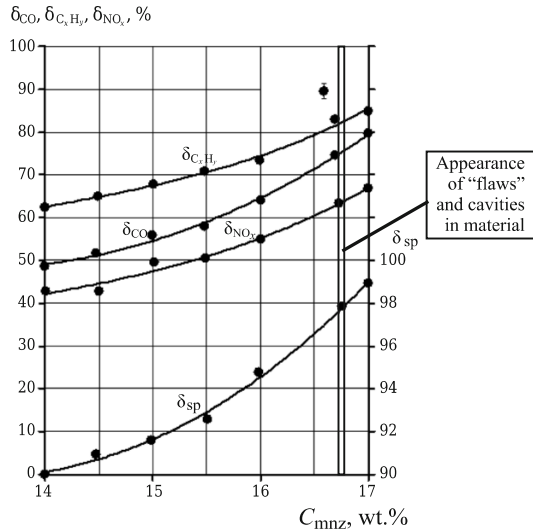


Fig. 8. Effect of  $C_{mnz}$  on exhaust gas cleaning quality at 850 K in SHS-material.

from 90 to 99%. However, a limitation of catalytic materials respect to quality makes it possible with dispensing 16.5% monazite to have a cleaning quality with respect to TP of 97%, 72% for carbon monoxide, 89% for hydrocarbons, and 50% for nitrogen oxides. Therefore, it has been confirmed that with monazite present within the SHS material composition catalytic properties develop in oxidation reactions for incomplete combustion products: solid particle (soot), carbon monoxide, and hydrocarbons, and also in reducing reactions for nitrogen oxides.

As a result of treating experimental material analytical dependences have been obtained connecting gas cleaning efficiency at 850 K with monazite content in a charge:

$$\delta_{TU} = 0.7334 \cdot C_{mnz}^2 - 19.78 \cdot C_{mnz} + 223.3, \quad (12)$$

$$\delta_{TU} = 2.316 \cdot C_{mnz}^2 - 61.732 \cdot C_{mnz} + 459.46, \quad (13)$$

$$\delta_{TU} = 1.5 \cdot C_{mnz}^2 - 39.011 \cdot C_{mnz} + 314.92, \quad (14)$$

$$\delta_{TU} = 1.5766 \cdot C_{mnz}^2 - 40.758 \cdot C_{mnz} + 303.96. \quad (15)$$

Therefore, it has been shown that replacement of cerium and thorium within a charge composition for catalytic materials by milled monazite ore within the limits of 17 wt.% makes it possible to obtain a high degree of exhaust gas cleaning from harmful substances. Experiments for evaluation of a catalytic neutralizer with SHS filters in a bus with a diesel engine showed that a reduction in nitrogen discharges at the start of testing was 61 – 62%, after 240 h of operation it was 62%, and 320 h of operation it was up to 66%; for car-

bon monoxide similar indices were 57 – 58, 47 – 48, and 45 – 46% respectively.

## CONCLUSION

1. Prerequisites have been established for using monazite in preparing PPCM by the SHS method exhibiting catalytic properties for cleaning diesel exhaust gases.

2. The effect has been considered of monazite content in a charge on pore size, porosity, and specific surface of SHS materials.

3. As a result of mathematical treatment of experimental material expressions have been obtained describing the dependence of specific surface, porosity, and sinuosity of pore diameter on monazite content in a charge for preparing SHS catalytic material.

4. It has been demonstrated that monazite as a catalyst may successfully replace expensive REE.

## REFERENCES

1. A. G. Merzhanov, *Self-Propagating High-Temperature Synthesis: 20 Years of Search and Discovery* [in Russian], ISMAN, Chernogolovka, (1989).
2. V. E. Ovcharenko, O. P. Solonenko, A. E. Chesnokov, and V. M. Fomin, "Effect of high energy reaction on the microstructure of synthesized cermet," *Pisma ZhTF*, **39**(21), 77 – 94 (2012).
3. V. E. Ovcharenko, O. V. Lapshin, O. P. Solonenko, et al., "High-temperature synthesis of cermet alloy in a powder mixture of mechanically activated metal components," Proc. IV All-Russia Conf. "Interaction of highly concentrated streams of energy with materials in prospective technology and medicine," Nonparel', Novosibirsk (2011).
4. A. A. Zenin and G. A. Nersisyan, *Chemistry and Physics of Combustion and Explosion. Combustion of Condensed and Heterogeneous Systems* [in Russian], ISMA, Chernogolovka (1980).
5. E. A. Levashov, A. S. Rogachev, V. I. Yukhvid, and I. P. Borovitskaya, *Physicochemical and Technological bases of Self-propagating High-Temperature Synthesis* [in Russian], BINOM, Moscow (2000).
6. V. V. Evstigneev and E. M. Belov (editors), *Self-propagating High-Temperature Synthesis. Materials and Technology* [in Russian], Nauka, Moscow (2001).
7. M. A. Kolomeets, A. V. Maetskii, T. V. Novoselova, et al., "Porous SHS-materials based on iron oxide and aluminum with additions of alloying elements," *Refract. Indust. Ceram.*, **58**(3), 293 – 298 (2017).
8. A. S. Noskov and Z. P. Pai, *Production Methods for Protecting Atmospheres from Harmful Discharges in Power generation Enterprises* [in Russian], SO RAN, GPNTB, Novosibirsk (1996).
9. T. V. Novoselova, N. N. Gorlova, G. V. Medvedev, et al., "Use of monazite ore in preparing porous permeable catalytic materials with high-temperature synthesis for cleaning diesel exhaust gases," *Izv. Tomsk Politekh. Univ.*, No. 3, 150 – 154 (2015).
10. T. V. Novoselova, D. S. Pechennikova, and A. E. Baklanov, "Cleaning diesel exhaust gases in catalysts based on monazite ore," *Polzunov. Vestnik*, No. 3 / 1, 158 – 161 (2012).

11. A. E. Baklanov, O. E. Baklanova, M. S. Kanapinov, et al., *SHS Materials for Cleaning Diesel Exhaust Gases: Monograph* [in Russian], VKGTU, Ust'-Kamenogorsk (2016).
12. A. E. Baklanov, M. S. Kanapinov, S. A. Malashina, et al., "Preparation of porous permeable materials using polymetal ore instead rare-earth elements," *Polzunov. Vestnik*, No. 2, 205 – 212 (2016).
13. V. V. Evstigneev, A. A. Geineman, V. I. Prolubnikov, and N. P. Tubalov, "Porous permeable materials in the iron oxide, silicon oxide, aluminum system," *Perspekt. Materialy*, No. 1, 69 – 72 (2007).
14. N. L. Chun and L. C. Shyan, "Combustion synthesis of aluminum nitride powder using additives," *J. Mater. Res.*, **16**, 2200 – 2208 (2001).
15. L. C. Shyan and H. L. Chun, "Combustion synthesis of aluminum nitride," *Key Eng. Mater.*, **521**, 101 – 111 (2012).
16. N. P. Tubalov, O. A. Lebedeva, and V. I. Vereshchagin, "Porous composite ceramic materials produced by a self-propagating high-temperature synthesis in the  $\text{Fe}_2\text{O}_3\text{-Al}_2\text{O}_3\text{-Al}$  system," *Refract. Indust. Ceram.*, **44**(5), 343 – 345 (2003).
17. V. I. Vereshchagin, V. V. Evstigneev, D. V. Kolesnikov, et al., "Self-propagating high-temperature synthesis technology for preparation of porous permeable materials," *Refract. Indust. Ceram.*, **46**(6), 416 – 418 (2003).